IEEE Access
Multidisciplinary | Rapid Review | Open Access Journal

Received 26 September 2024, accepted 22 October 2024, date of publication 28 October 2024, date of current version 5 November 2024.

Digital Object Identifier 10.1109/ACCESS.2024.3486792

RESEARCH ARTICLE

Indoor Area Estimation System Using RSSI-Measuring Handheld Reader Utilizing Directional Reference RFID Tags and Machine Learning

DANANG KUMARA HADI[1,2], ZEQUN SONG[1], BUDI RAHMADYA[3], (Member, IEEE), SHOGO KOZUME[1], TOMONORI SUMIYA[1], RAN SUN[4], (Member, IEEE), SHIGEKI TAKEDA[4], (Member, IEEE), AND XIAOYAN WANG[4], (Senior Member, IEEE)

[1]Graduate School of Science and Engineering, Ibaraki University, Hitachi, Ibaraki 316-8511, Japan
[2]Department of Agroindustrial Technology, Universitas Muhammadiyah Jember, Jember 68124, Indonesia
[3]Computer System Department, Faculty of Information Technology, Andalas University, Padang 25175, Indonesia
[4]College of Engineering, Ibaraki University, Hitachi, Ibaraki 316-8511, Japan

Corresponding author: Shigeki Takeda (shigeki.takeda.tmkyou@vc.ibaraki.ac.jp)

This work was supported by the Japan Science and Technology Agency (JST) establishing University Fellowships Toward Creating Science and Technology Innovation under Grant JPMJFS2105.

ABSTRACT Achieving efficient warehouse operations for product management in an indoor environment has recently become a challenging issue. If a user can store a product in a vacant place and then roughly localize the product with a simple system, this localization system will enable efficient and flexible area usage in a warehouse. Complex radio wave propagation phenomena also make indoor localization more challenging. This paper introduces a radio frequency identification (RFID) system to localize products in indoor environments, including warehouses and cold storage. This approach uses distributed directional reference RFID tags in the areas as product location beacons, enabling received signal strength indicator (RSSI) measurements reflecting information on distances and directions for determining product coordinates. A user with a handheld reader stands in the close vicinity of the product. Then, the user reads the surrounding reference RFID tags for collecting the RSSI data. The use of machine learning (ML) addresses unstable user behaviors and unexpected acquired RSSI variations due to wireless propagation. Regression and classification algorithms in ML estimate product locations. The experimental demonstrations in actual indoor environments validate the proposed localization method. The experimental environments measure $24\,m \times 12\,m$ in a conference room and $9\,m \times 12\,m$ in a laboratory room. Experimental results show that this approach can provide localization accuracy of less than 2 meters, with wide application potential in inventory management and product tracking in various indoor environments, including factories, warehouses, and cold storage.

INDEX TERMS Handheld reader, indoor area, inventory management, machine learning, RFID tags, RSSI.

I. INTRODUCTION

Presently, the localization system of products has become increasingly popular in recent years due to its ability to provide real-time location data for various applications, such as fleet management [1], [2], asset tracking [3], [4], [5], [6] and personal safety [7]. These products typically use a combination of global positioning system (GPS), cellular, and Wi-Fi technologies [8], [9] to provide accurate location data. In industrial applications, this system is utilized for supply chain traceability [10], [11], [12] and increasing efficiency in manufacturing processes [13], [14]. These systems are designed to track the movement of products throughout the manufacturing process, from raw materials to finished goods, and to provide real-time insights into inventory levels [15], [16], production processes [17], shipping and

The associate editor coordinating the review of this manuscript and approving it for publication was Nurul I. Sarkar.

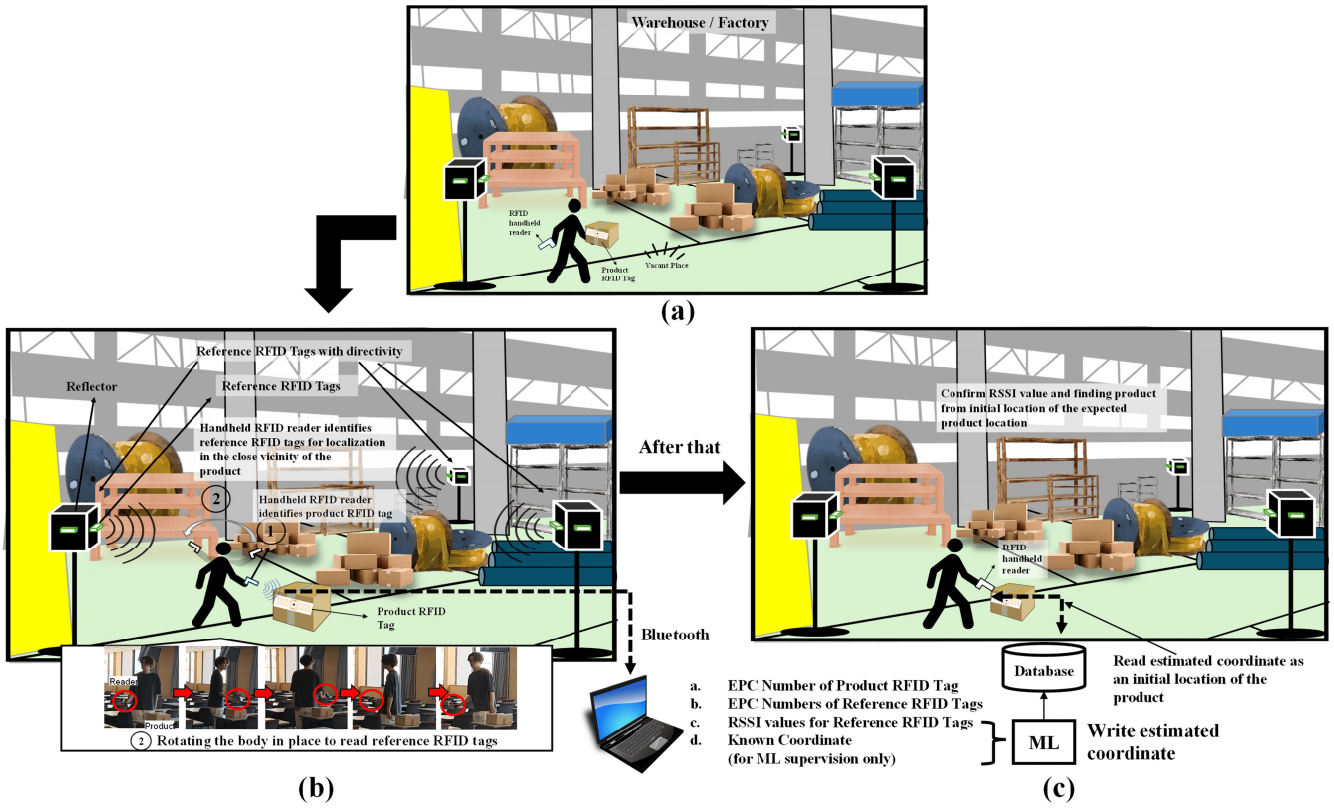

FIGURE 1. Products management and their localization mechanisms using RFID tags. Product RFID tags enable item-level product management. Reference RFID tags with directivities facilitate the localization of the products. The database combines the estimated coordinates with the EPC of the product RFID tags. This localization makes it possible to search for a specific product on demand. This system consists of three procedures: (a) placing a product with a product RFID tag in a vacant area, (b) localizing this area using reference RFID tags, a handheld RFID reader, and ML, (c) searching for the product on a demand basis by reading the estimated coordinate from the database.

delivery schedules [18]. Industrial product tracking systems with their features and benefits are available today [19]. Popular product tracking systems include barcode scanning, GPS [20], and radio frequency identification (RFID) systems. RFID systems use small electronic tags to track products through the supply chain [21], providing real-time data on the location and status of the products [22]. Furthermore, GPS is unsuitable for indoor positioning [23]. To address this limitation, ultra-high-frequency (UHF) band RFID technologies enable tracing of the locations of indoor products. UHF band RFID tags can be read at a distance of several meters to tens of meters between an RFID reader and RFID tags [24], [25], [26].

Recently, the development of RFID localization systems in industry today has had a significant impact and is increasingly showing great potential for transformation in various fields. Product localization systems based on RFID in the indoor industry provide real-time location data and visibility of products as they move through the supply chain [27], [28] from manufacturing to delivery [29], [30], [31]. The use of received signal strength indicator (RSSI) and phases is possible for RFID-based localization. RSSI is a convenient choice for localization because some commercially available RFID readers only measure RSSIs. By providing real-time tracking information, product tracking systems [32] can help businesses identify and address bottlenecks or delays in the supply chain [33], optimize inventory levels [34], and improve customer services [22]. These systems can reduce costs and energy for decarbonization [35], increase productivity, and improve user satisfaction. RFID-based localization systems can benefit by using device-free technologies that do not require additional devices to be worn on humans [36], [37].

This paper proposes the localization method of storing goods in the warehouse using directional reference RFID tags, a handheld RFID reader, and machine learning (ML). The RFID tags have directivities, and ML facilitates localization in complex indoor environments. The proposed method focuses on indoor localization to overcome GPS constraints and multipath challenges caused by complex variations in the received signal strength indicator (RSSI). Experimental results in actual indoor environments validate the purpose method. The users read neighboring reference RFID tags for localization using a handheld RFID reader to obtain RSSI values. Directional reference RFID tags can overcome the effects of multipath fading and improve positioning accuracy. The reference RFID tags also provide angle information. Applying ML to understand complex trends in the RSSI value can significantly improve positioning accuracy in indoor environments.

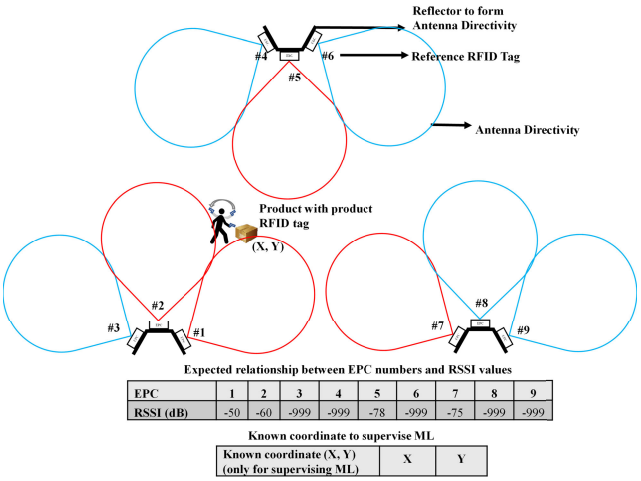

Expected relationship between EPC numbers and RSSI values

EPC	1	2	3	4	5	6	7	8	9
RSSI (dB)	-50	-60	-999	-999	-78	-999	-75	-999	-999

Known coordinate to supervise ML

Known coordinate (X, Y) (only for supervising ML)	X	Y

FIGURE 2. Role of reference RFID tags and the structure of a dataset for ML.

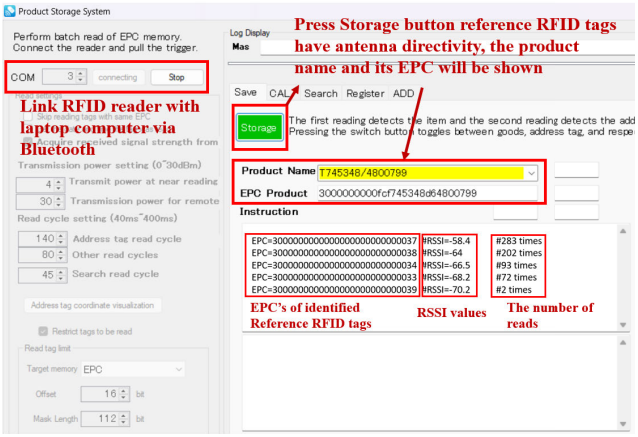

FIGURE 3. RFID reader control software.

This paper is organized as follows: Section II proposes a localization system using a handheld RFID reader, directional reference RFID tags, and ML for inventory management. Section III discusses the experimental environment and validation conditions. The experimental results in Section IV cover the accuracy and reliability of the ML system in determining the position of indoor products, including maximum error measurements, error distribution, and the required number of datasets for supervising ML. Section V concludes this paper.

II. PROPOSED PRODUCTS MANAGEMENT AND THEIR LOCALIZATION METHOD

This section explains the proposed product management and its localization mechanism. The proposed RFID-based localization system assumes the use of a handheld RFID reader and reference RFID tags for flexible product management in indoors. The handheld RFID reader obtains the electronic product code (EPC) numbers and RSSI values. The proposed system only uses this basic information to localize a product in a warehouse, thereby making the proposed method versatile and simple because most commercially available RFID readers can measure RSSI values.

Figure 1 shows an operational principle of product management and their localization method. In Fig. 1 (a), a user places a product at a vacant place the floor in a warehouse and factory, and identifies a product RFID tag appended to the product by using a handheld RFID reader. In Fig. 1 (b) the user subsequently localizes the product. Because the user is in the close vicinity of the product, this localization enables product localization. The proposed system uses RFID tags to implement these two functions: a product RFID tag for item-level product management and a reference RFID tag used to localize the product in a warehouse.

The procedure of this system consists of three stages. The user first places a product having an RFID tag for item-level identification in a vacant area, as shown in Fig. 1 (a). This system subsequently performs area localization using reference RFID tags, a handheld RFID reader, and a Machine Learning (ML) approach as in Fig. 1 (b). The ML processes the RSSI information of the reference RFID tags for area estimations. The database keeps the estimated coordinate. After this, the system reads the estimated product coordinates from the database as an initial coordinate for searching and localizing the product on a demand basis, as shown in Fig. 1 (c). A user searches and localizes the product RFID tag with the handheld RFID reader by monitoring the signal levels of the product RFID tag.

This paper focuses on the area estimation method, as shown in Fig. 1 (b).

The antenna of the reference RFID tag has specific directivity. A reflector allows an antenna to have perpendicular directivity.

The directivity of the reference RFID tag enables the proposed localization method to estimate angles. In addition, this directivity enables RSSI variations caused by multipath propagation to be mitigated while improving the direct propagation path [38]. This directivity also leads to long read distances. Angularly sectorized reference RFID tags distributed in a warehouse enable the localization of products. The following section details the specific allocations of the reference RFID tags in the experimental environments considered in this paper.

Note that the reference RFID tags are installed in known places. The user identifies the reference RFID tags with a handheld RFID reader by moving the arm while rotating the body in place. This reading method facilitates reliable reference RFID tag identification. Reliable identification of reference RFID tags enhances localization accuracy because the localization system can acquire detailed information on RSSI decay and the incident angles of radio waves.

Despite the use of directional antennas, swinging the arm and rotating the body in place may cause unexpected variations in the obtained RSSI information. The remaining multipath propagation effects still cause RSSI variations.

ML compensates for these unstable phenomena, making the proposed localization method robust and reliable. The

next section details the implementation of the ML algorithms. After training, the ML method processes the ordered RSSI values of identified reference RFID tags to generate a predicted coordinate for the product. In the ML supervision phase, ordered RSSI values and a known coordinate or label are used to construct a dataset at each known location to facilitate ML supervision. The directional radiation patterns in the reference RFID tags reduce the number of datasets needed to enable the ML method to be trained because the directivities mitigate multipath fading effects.

A database links the EPC number in a product's RFID tag to its ML-generated coordinate for searching for the product on a demand basis.

Figure 2 shows examples of a reference RFID tag arrangement and its antenna directivities. As previously mentioned, after placing a product in a vacant space, the user identifies the product's RFID tag with a handheld RFID reader. The user subsequently identifies the surrounding reference RFID tags in the area with the same handheld RFID reader by swinging the arm and rotating the body. The reference RFID tags, with directivities indicated by red lines, will respond to requests issued by the handheld RFID reader. Depending on the angles and distances between the handheld RFID reader and reference RFID tags, the RSSI values are measured, and a dataset of ordered RSSI values is constructed, as shown in the upper table. Note that an RSSI value of −999 dB represents undetected reference RFID tags because numerically representing unidentified reference RFID tags simplifies the data representation and ML implementation.

In the learning phase, the ML method processes the RSSI values at known coordinates to allow ML supervision. The tables in Fig. 2 represent the format of the dataset. This learning phase uses the ordered RSSI values (upper table) and known coordinates (lower table). The datasets collected at known points in an area enable ML supervision. After this learning phase, the ML method generates a predicted coordinate based only on a dataset consisting of RSSI values. The following sections describe the proposed localization system.

Note that if the test datasets have reference RFID tags' position errors for the learning datasets, this situation will degrade localization accuracies. The changes in furniture arrangements will also cause degradation. Therefore, the updates of the learning datasets will be necessary. Additional reference RFID tag sets can enhance a coverage area.

If phase information is available, it allows accurate localization and synthetic aperture radar (SAR)-based self-localization and trajectory estimation for moving robots [19], [27], [39], [40], [41], [42]. Time-of-arrival (ToA)-based localization enables accurate localization. However, some commercially available RFID readers, including the handheld reader that was used in this paper, provide only RSSI information because the software development kit (SDK) and its software library do not support measurements of the phase and Doppler shift of radio waves. In this context, the proposed indoor localization method involves the use of reference RFID tags with directive antennas, instantaneous RSSI measurements, and ML to develop a versatile indoor localization method. The reference RFID tags with antenna directivities sectorize the indoor area, facilitating RSSI-based indoor localization. Furthermore, the use of ML and its learning overcome the inferior localization performance of indoor localization based on RSSI alone, especially in multipath-rich environments. The subsection shown later experimentally validates the effect of ML and how much the ML improves the localization performance on the basis of the distance decays of RSSI values [27], [28].

The purpose of the use of RFID was to develop a simple and easy-to-use area localization method to register the estimated area coordinate of an item to a database while eliminating human error, dependence on individual human skills and physical abilities, language barriers for international workers, time use inefficiencies, and manual data entry. In a local middle-scale factory environment in Japan, operations by human workers are realistic due to a limited budget and congested environment, both of which prohibit the introduction of highly accurate and fully automated robot-based or unmanned ground vehicle (UGV)-based item management. We also need to assume the presence of existing stored items on the floor, tall facilities and items, and stacked items. These items and facilities shadow the visual identification of optical markers and posters for localization. RFID is more robust for dirt on optical makers and posters indicating areas. Instantaneous RSSI values also increase the time efficiency of the proposed method. RFID systems eliminate manual data entry and careless mistakes.

III. EXPERIMENTAL SETUP AND ENVIRONMENTS

This section details an experimental setup and environments for validating the proposed localization method. The subsections each explain the reference of RFID tag specifications, experimental environments, an employed ML model, and the preparation of datasets for ML.

The experimental setup employed the RFID tags named Shortdipole produced by Avery Dennison. The RFID handheld reader used in this work was DOTR-3200, which radiates 1 W directional circularly polarized radio waves in a 920 MHz band. Bluetooth connected the handheld RFID reader to a laptop computer. RFID reader software developed in C# collected EPC numbers and the corresponding RSSI values of identified reference RFID tags. Fig. 3 shows a snapshot of the developed software on a laptop computer.

A. EXPERIMENTAL ENVIRONMENTS

Reference RFID tags employ metal plates as reflectors that create antenna directivities perpendicular to the reflectors. The use of reflectors increases the read distances of the reference RFID tags by increasing the antenna gains of the reference RFID tags. Figure 4 shows two types of reference RFID tags used in this study. The spacing between the metal plate and the reference RFID tag is $\lambda/4$ to create a single

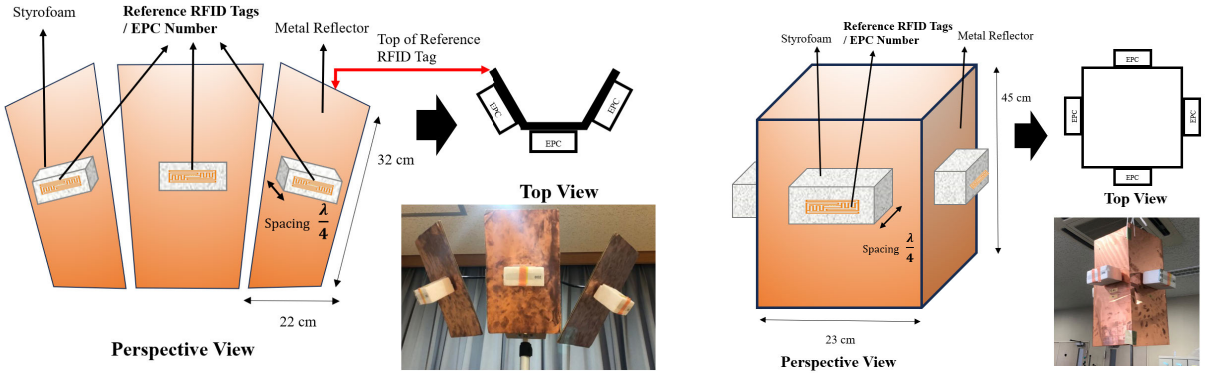

FIGURE 4. Reference RFID tags for experiments. (a) three directive antennas tilted to place them along the walls at higher heights and (b) four directive antennas for placing around the center areas of a room.

beam radiation pattern, where λ is a wavelength at 920 MHz. RFID tags are horizontally arranged. The reference RFID tags shown in Figs. 4 (a) and (b) have three directivities and four directivities, respectively. The reflectors shown in Fig. 4 (a) are tilted toward the floor so that these reference RFID tags are suitable for placing along walls at higher heights. The reference RFID tags enable us to estimate not only the distances but also the directions of the handheld RFID reader.

The moment-based electromagnetic simulator (EEM-MOM ver. 3.0) was used to compute the radiation pattern of the reference RFID tag; the antenna geometry of the reference RFID tag was constructed by referring to the actual Avery Dennison Shortdipole. Figure 5 (a) shows the geometry of the reference RFID tag, and Figs. 5 (b) and (c) compare the antenna radiation patterns of the reference RFID tag without and with the tilted reflector at a tilt angle of 45°. The horizontally oriented reference RFID tag antenna without the tilted reflector, approximated as a dipole antenna, has an omnidirectional radiation pattern in the elevation plane, as shown in Fig. 5 (b). In contrast, the reference RFID tag with the tilted reflector creates a single-beam radiation pattern toward the ground, yielding an antenna radiation pattern in the elevation plane, as shown in Fig. 5 (c). Accordingly, the reflectors provided 5.41 dB antenna gain increases, enabling more sensitive and long-range RSSI measurements.

The spacing between the reference RFID tag and its reflector was a quarter of the wavelength [43] at an operating frequency of 920 MHz to create single-beam radiation. A reflector with this spacing increases the antenna gain with less degradation of impedance matching.

The reflectors behind the reference RFID tags enhance their reading distances, thereby expanding the coverage of the reference RFID tags. According to Friis's transmission formula, the gain increase (5.41 dB) obtained in the analyses shown in Figs. 5 (b) and (c) increases the reading distance $\sqrt{3.5} = 1.87$ times. Therefore, reference RFID tags with reflectors can reduce the number of reference RFID tag sites available for covering a localization area.

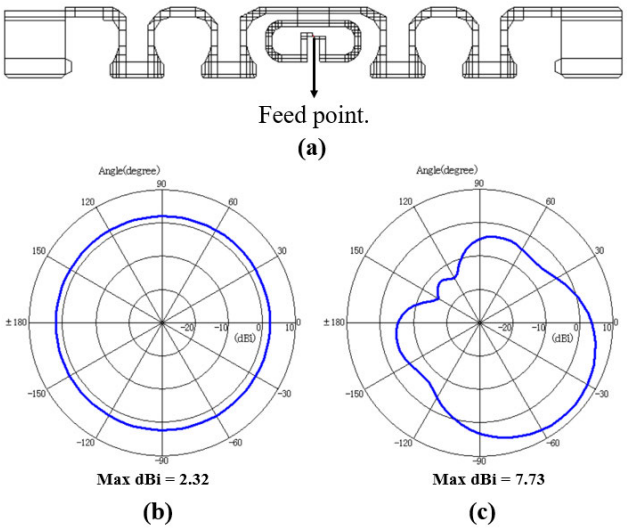

FIGURE 5. Reference RFID tag antenna geometry and radiation patterns in the elevation plane without and with the tilted reflector. (a) Reference RFID tag antenna geometry without the tilted reflector, (b) radiation pattern (without the tilted reflector), and (c) radiation pattern (with the tilted reflector, at a tilt angle of 45 °).

The experimental environments include a conference room and laboratory room at Ibaraki University. The conference room is located in Building E5 on the 8th floor and measures $24\,m \times 12\,m$. The laboratory room is located in Building E5 on the 4th floor and measures $9\,m \times 12\,m$. Three sets of the reference RFID tags shown in Fig. 4 (a) cover the conference room using nine reference RFID tags. Three reference RFID tag sets shown in Fig. 4 (b) also cover the laboratory room using 12 reference RFID tags. Figs. 6 and 7 show the experimental environments.

The room shown in Fig. 6 is a conference room and equips tables and chairs. The sets of reference RFID tags shown in Fig. 4 (a) were placed along the walls at three locations. Because there are no tall metallic objects, the propagation between the handheld RFID reader and reference RFID tags comprises line of sight (LoS) channels. The localization results in this environment serve as reference data for the

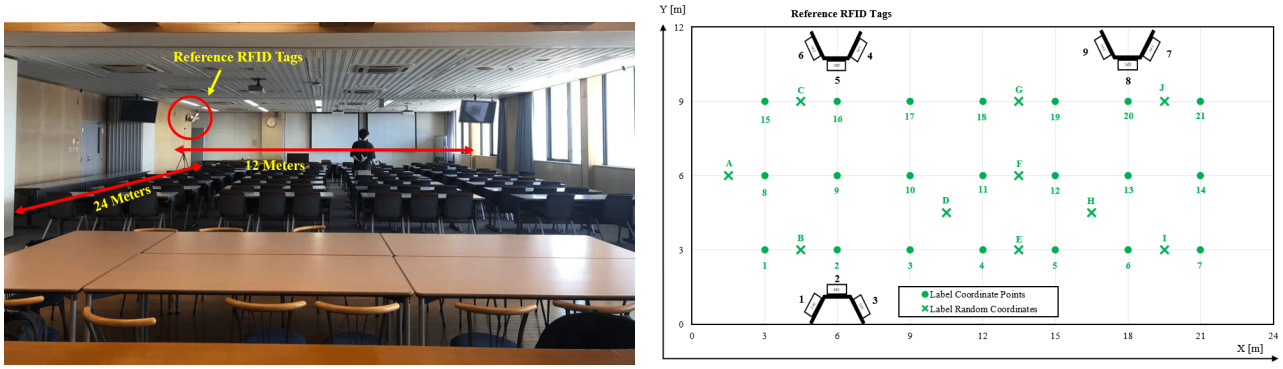

(a) (b)

FIGURE 6. Experimental setup and environment of a conference room. (a) photo of the conference room and (b) layout of the reference RFID tags and points for ML training and evaluation.

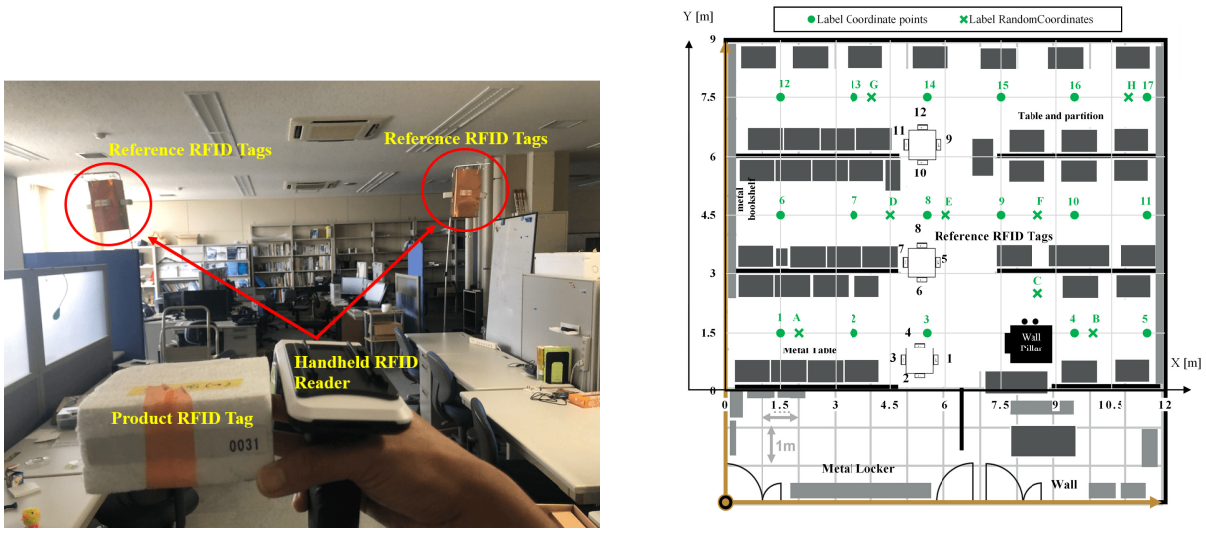

(a) (b)

FIGURE 7. Experimental setup and environment for a laboratory room. (a) photo of the laboratory room and (b) layout of the reference RFID tags and points for ML training and evaluation.

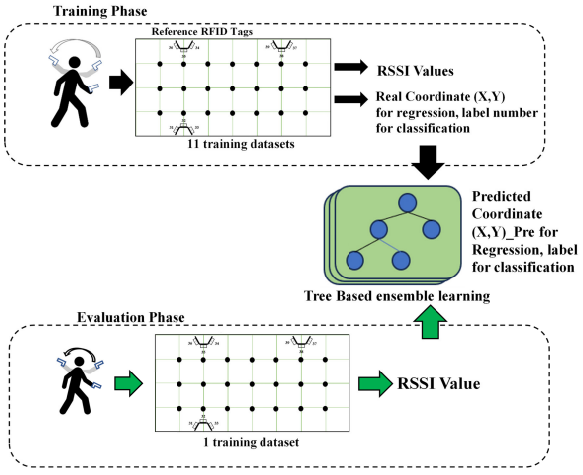

FIGURE 8. Procedure for ML training and evaluation in the conference room.

system validation in this paper. The circles in this figure represent the points to obtain the data for ML supervision. The spacing between the points is three meters. The height of the reference RFID tags is 2.3 meters, whereas that of the ceiling is 2.5 meters. The crosses show randomly chosen coordinates for validating the versatility of the proposed localization method.

The laboratory room shown in Fig. 7 has many high metallic partitions and a large pillar. This environment causes complicated radio wave propagation channels, sometimes leading to non-line-of-sight (NLoS) propagation channels. This room provides a realistic evaluation environment as warehouses and cold storage to validate the proposed method. The height of the reference RFID tags was two meters. Furthermore, randomly chosen points represented by crosses in Fig. 7 evaluated the versatility of an ML algorithm.

The numbers and alphabets represent the labels utilized for evaluating classification algorithms later.

The conference room and laboratory are assumed to be environments with no major existing facilities and a congested area, respectively. These environments partly simulate factory and warehouse environments. Although this

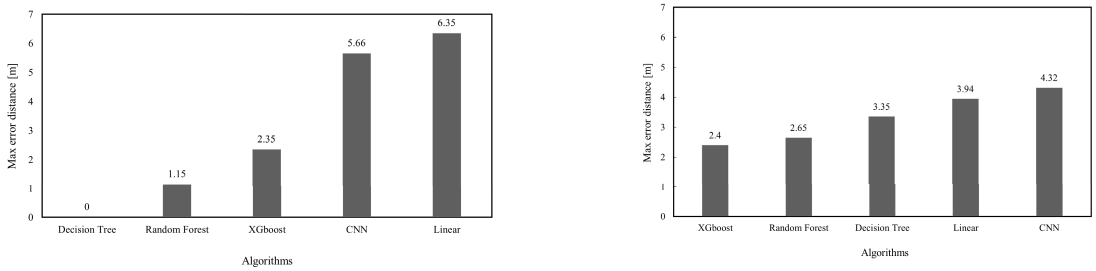

FIGURE 9. Comparative studies of typical ML algorithms in terms of the maximum error distances in the conference room: (a) on-grid coordinates and (b) off-grid random coordinates.

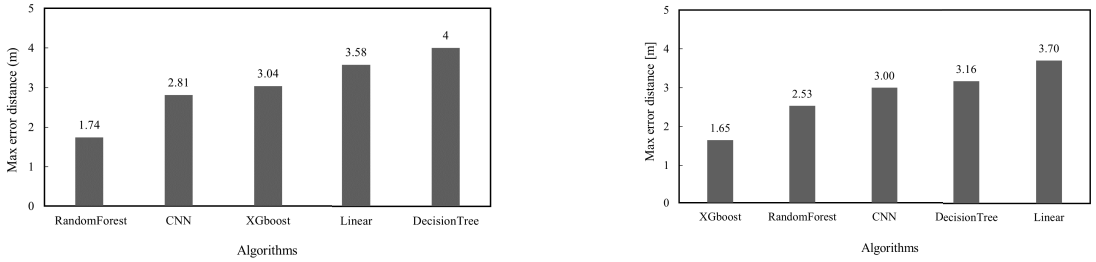

FIGURE 10. Comparative studies of typical ML algorithms in terms of the maximum error distances in the laboratory room: (a) on-grid coordinates and (b) off-grid random coordinates.

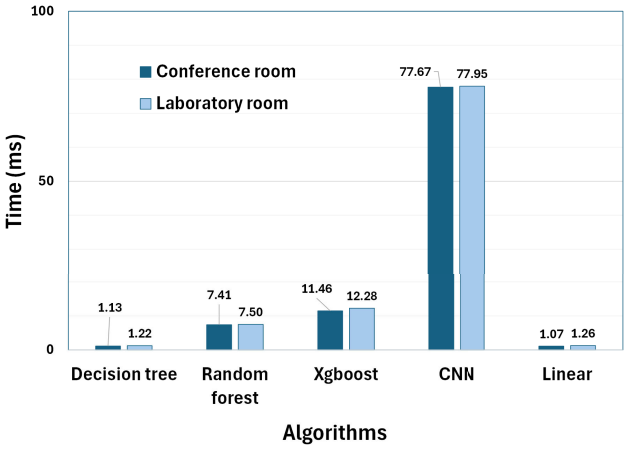

FIGURE 11. Average processing times for the individual ML algorithms.

paper assumes that items are stored in a vacant area on the floor, as shown in Fig. 1, if environments have equally spaced tall metallic shelves, the arrangement scenarios of the reference RFID tags need to be modified because the shelves may shadow the radio wave propagation paths. An evaluation of this environment will be performed in the future.

This paper evaluated our method in indoor environments to determine how the proposed method overcomes and addresses multipath effects in indoor environments. An inverse distance weight (IDW)-assisted particle swarm optimized (PSO) indoor localization (IDWPSOInLoc) [44] was used to evaluate a wireless fidelity (WiFi)-based indoor localization method in a 57-m wide indoor corridor area. Although the experimental environment in this paper is sometimes narrower than warehouses and factory environments, our experimental environment partly mimics real environments. Furthermore, narrower indoor environments cause severe multipath effects and are suitable for assessing the robustness of the proposed method for indoor multipath effects. In addition, the proposed method can widen the coverage of the proposed method by deploying additional reference RFID tags and applying them to the environment in [44]. Our future work will include detailed evaluations of the proposed method in larger indoor areas.

B. PROCEDURES FOR TRAINING AND EVALUATING ML

Python libraries named scikit-learn enabled ML processing. Figure 8 shows ML procedures assuming the use of a tree-based ensemble learning. The proposed system collects the datasets on the points by performing the procedures explained in Figs. 1 and 2 multiple times to supervise ML. The obtained datasets were divided into two datasets, enabling ML training and evaluation. The data consist of ordered RSSI values of the identified reference RFID tags and known coordinates (X, Y) in the ML training phase. These datasets facilitate supervision of ML in the experimental environments.

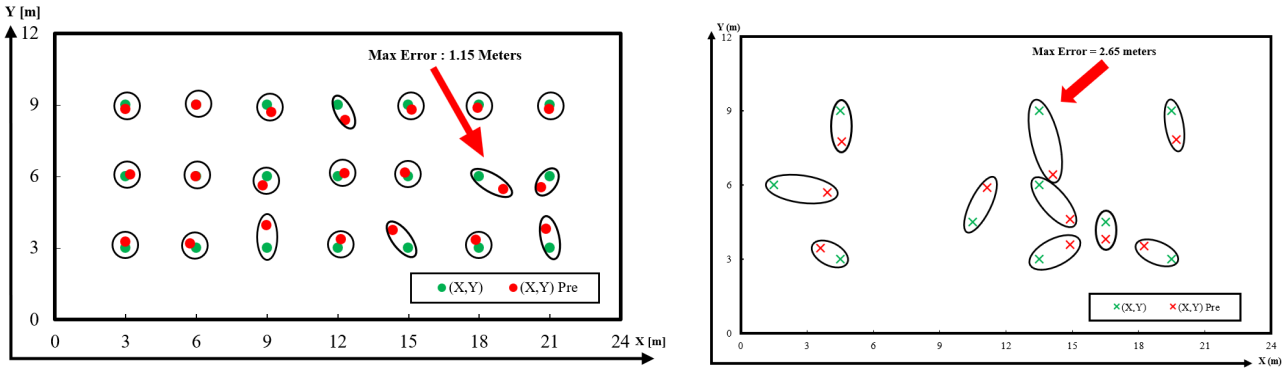

(a) (b)

FIGURE 12. Maximum error distance maps in the conference room using a random forest algorithm: (a) on-grid coordinates and (b) randomly chosen off-grid coordinates.

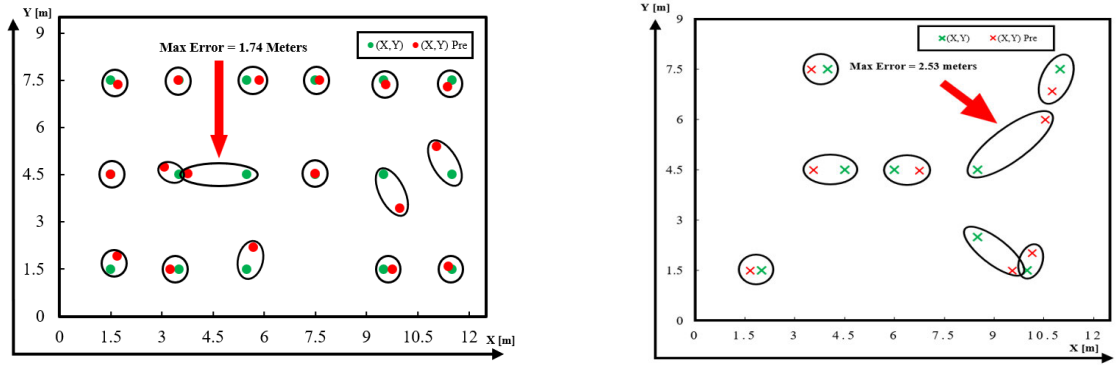

(a) (b)

FIGURE 13. Maximum error distance maps in the laboratory room using a random forest algorithm: (a) on-grid coordinates and (b) randomly chosen off-grid coordinates.

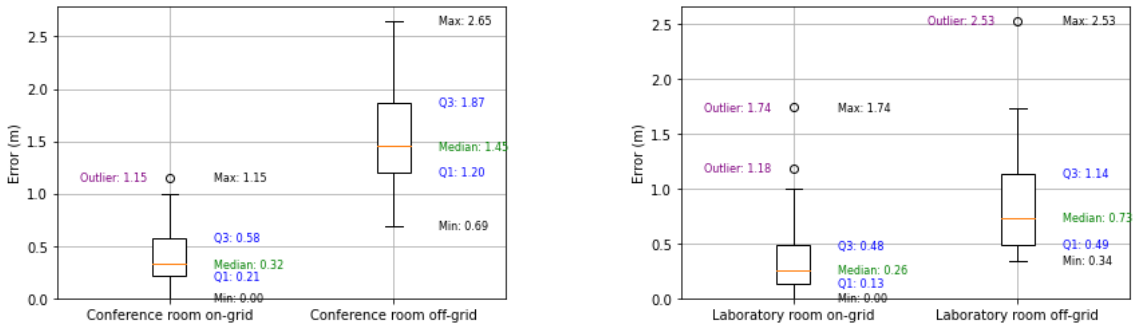

(a) (b)

FIGURE 14. Box-and-whisker plots for error distances obtained by regressions with random forest algorithm: (a) Conference room at on-grid and off-grid and (b) Laboratory room at on-grid and off-grid.

The data consist of ordered RSSI and coordinates (X, Y) in the ML training phase for use in regression algorithms. In the classification, the location is learned and predicted by referring to the RSSI values and position labels.

C. PREPARATION OF DATASETS FOR ML TRAINING AND EVALUATION

There were 21 points with an interval distance of 3 meters in the conference room, as shown in Fig. 6. The experiments were conducted in the conference room twelve times on each of the 21 points. Eleven datasets for training and one dataset for testing on each of the 21 points are utilized for ML training and evaluation, respectively.

The laboratory room has 17 points with a distance interval of 1.5 meters, as shown in Fig. 7. The experiments in this room collected 16 datasets at each of the 17 points of training and one dataset for testing because this room contains many pieces of high-tall metallic furniture. Sixteen datasets and one dataset were employed for ML training and evaluation, respectively. Because severe multipath fading may cause unexpected variations in RSSI values, the number

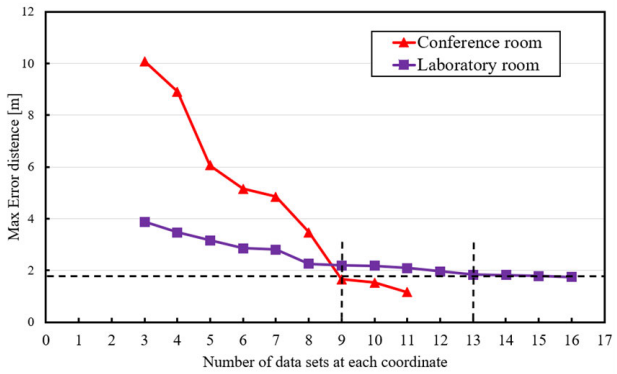

FIGURE 15. Maximum error distance as a function of the number of datasets.

of datasets in the laboratory room, 17, is greater than that in the conference room, 12.

IV. EXPERIMENTAL RESULTS

A. EVALUATION OF MAXIMUM ERRORS FOR TYPICAL ML-BASED REGRESSION ALGORITHMS

The evaluation results for typical ML algorithms enable identification of the most suitable algorithm for our localization environments. This paper evaluated a random forest algorithm [45], XGBoost algorithm [46], decision tree [47], linear regression [48], and convolutional neural network algorithm (CNN) [49]. Figures 9 and 10 provide comparative studies on the maximum error distances for ML algorithms at the coordinates presented in Figs. 6 and 7, respectively. The required number of datasets for ML will be clarified in the subsequent subsection. In addition, Figs. (a) and (b) in each figure respectively provide maximum error distances on the points for supervising ML (on-grids) and randomly chosen coordinates for evaluating the versatilities of individual ML algorithms (off-grids). Note that the maximum error distance is the largest error distance for each algorithm.

From Figs. 9 (a) and (b), although the decision tree provided the best localization performance for on-grid points in the conference room as shown in Fig. 9 (a), this algorithm was not versatile enough because the maximum error provided for off-grids was not minimum as shown in Fig. 9 (b). Furthermore, the decision tree algorithm was worse for the on-grid and off-grid points in the laboratory room, as discussed in the following figure. On the other hand, the XGBoost provided the best performance for the off-grid points. This algorithm, however, did not achieve the best performance for the on-grid points. The linear regression and CNN algorithms were worse in the conference room. The random forest algorithm provided the second-best performance for both on- and off-grid coordinates.

As shown in Figs. 10 (a) and (b), we can confirm that using the random forest was the best choice for the laboratory room. Although in Fig. 10 (b) XGboost has good performance on off-grid, this algorithm has a large error, as shown in Fig. 10 (a). The decision tree, CNN, and linear regression algorithm were worse for the on-grid and off-grid points.

These evaluation results confirmed that the random forest algorithm was suitable for regression in this experimental environment.

To evaluate the latencies of the ML methods, Fig. 11 shows the average processing times of the individual ML methods over the on-grid points in each room, where the processing time corresponds to the time between introducing the RSSI vector and generating the predicted coordinate in the evaluation phase, as shown in Fig. 8. The specifications of the computer were as follows: Windows 11 Pro 64-bit, 13th Gen Intel Core i7-1355U (12 CPUs), 2.6 GHz, 32 GB RAM. The processing times for the laboratory are longer than those for the conference room because the laboratory has more reference RFID tags than the conference room does, which makes the input vector of RSSI values to the MLs large.

B. MAXIMUM ERROR DISTANCE DISTRIBUTIONS FOR RANDOM FOREST REGRESSION ALGORITHM

Because we confirmed that the random forest regression was the most suitable for our experimental environments, the error distance distribution maps for the random forest algorithm further evaluate the localization performance of the proposed method. Figures 12 and 13 show the error distance distribution maps for the conference room and laboratory room, respectively. Figures (a) and (b) show the results for the on- and off-grid coordinates, respectively. The red and green symbols represent the ideal and predicted coordinates, respectively. These results confirmed that the proposed localization system works well in realistic indoor environments.

Figures 14 (a) and (b) show box-and-whisker plots presenting the detailed information, including means and deviations, for Figs. 12 and 13, respectively.

Considering the use of an unstable handheld RFID reader operated by human workers, the use of instantaneous RSSI values, congested and multipath indoor environments, and the search procedure that is used when inventorying the expected items, the obtained distance errors are acceptable for managing items in a local factory in Japan. The search capability of the RFID system shown in Fig. 1 can inventory the expected items and absorb the inadequate accuracies of the proposed method. These points make the proposed system acceptable despite its modest accuracies.

C. NECESSARY NUMBER OF DATASETS FOR SUPERVISING ML

Collecting datasets for supervising ML is a time-consuming and labor-intensive task. Therefore, clarifying the number of necessary datasets for supervising ML is crucial. Figure 15 shows the maximum error distance as a function of the number of datasets at each coordinate for the conference and laboratory rooms. These results confirmed that the maximum error distances saturate at nine and thirteen for the conference

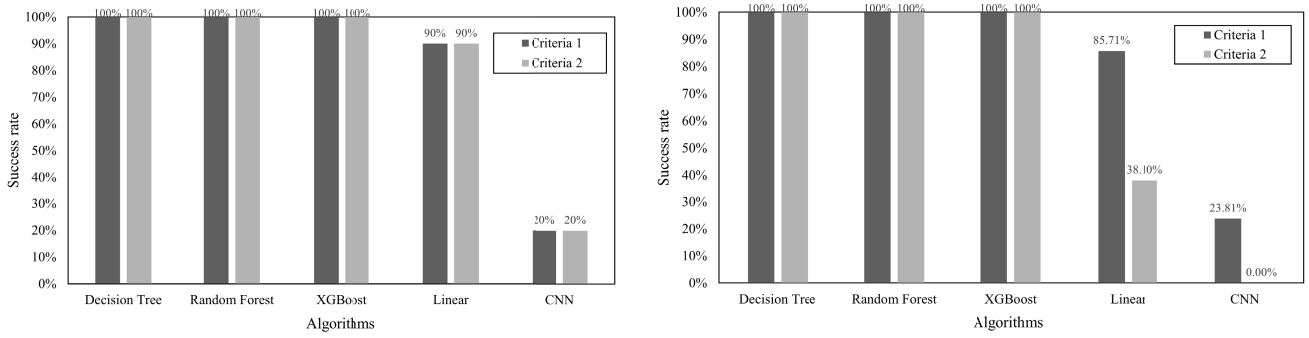

(a) (b)

FIGURE 16. Success rates for classifications in the conference room: (a) on-grid and (b) off-grid.

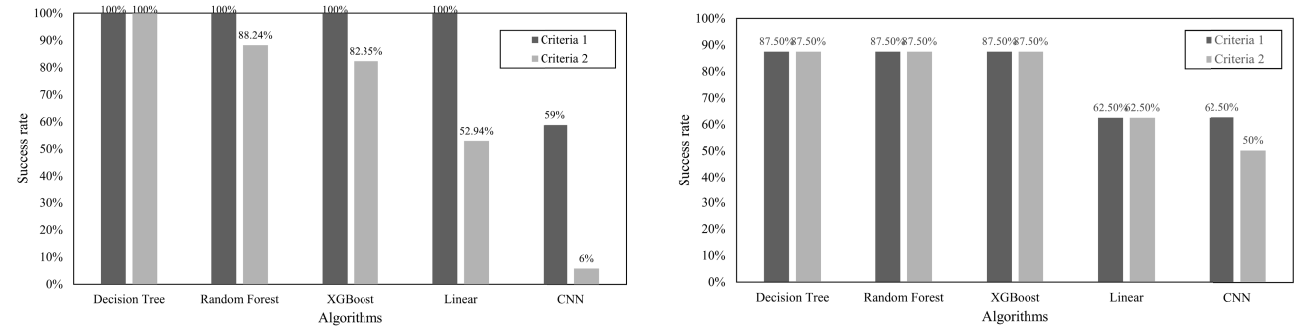

(a) (b)

FIGURE 17. Success rates for classifications in the laboratory room: (a) on-grid and (b) off-grid.

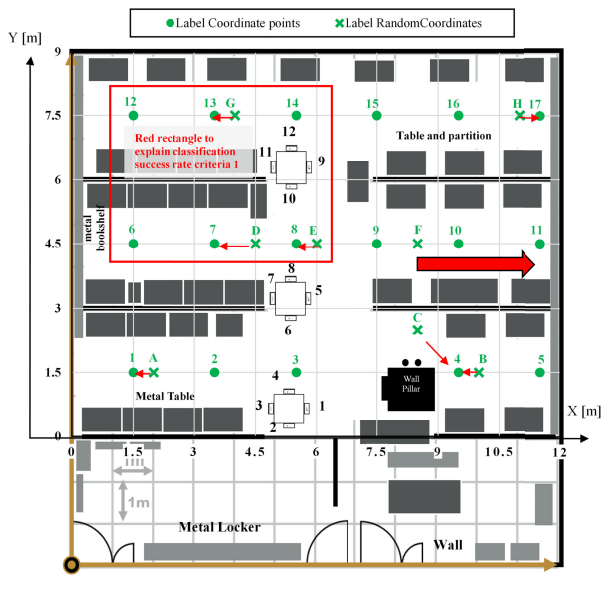

FIGURE 18. Error map of the laboratory room: off-grid using the decision tree algorithm.

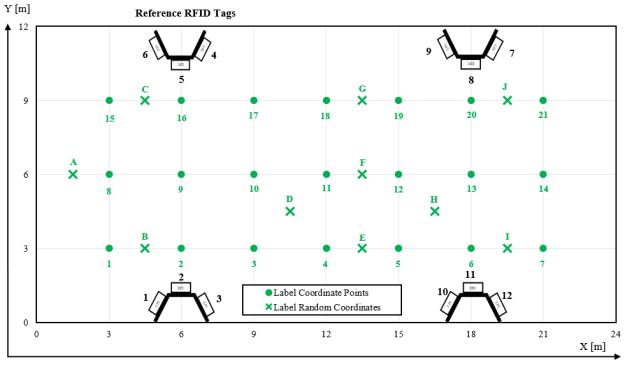

FIGURE 19. Experimental setup and environment of the conference room with 4 reference RFID tag sites and points for ML training and evaluation.

room and laboratory room, respectively. These necessary numbers are realistic for the practical implementation of the proposed method.

Figure 15 also shows the RSSI variations among the datasets obtained at the same data acquisition positions. The relationships between the maximum error distances and the number of datasets at each coordinate confirmed that increasing the number of datasets at each coordinate caused the maximum error distances to gradually decrease and converge to certain levels. These trends are due to the variations among the RSSI datasets obtained at the same data acquisition positions. Preparing nine and 13 RSSI datasets at the same data acquisition positions suppressed the effects of RSSI variations in the conference and laboratory rooms, respectively.

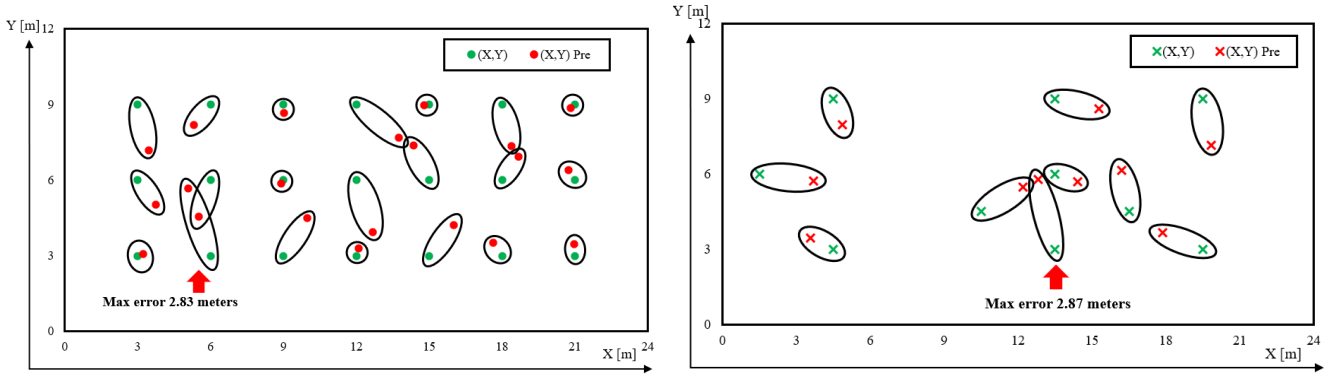

(a) (b)

FIGURE 20. Maximum error distance maps of the conference room using a random forest algorithm with (a) on-grid coordinates and (b) randomly chosen off-grid coordinates.

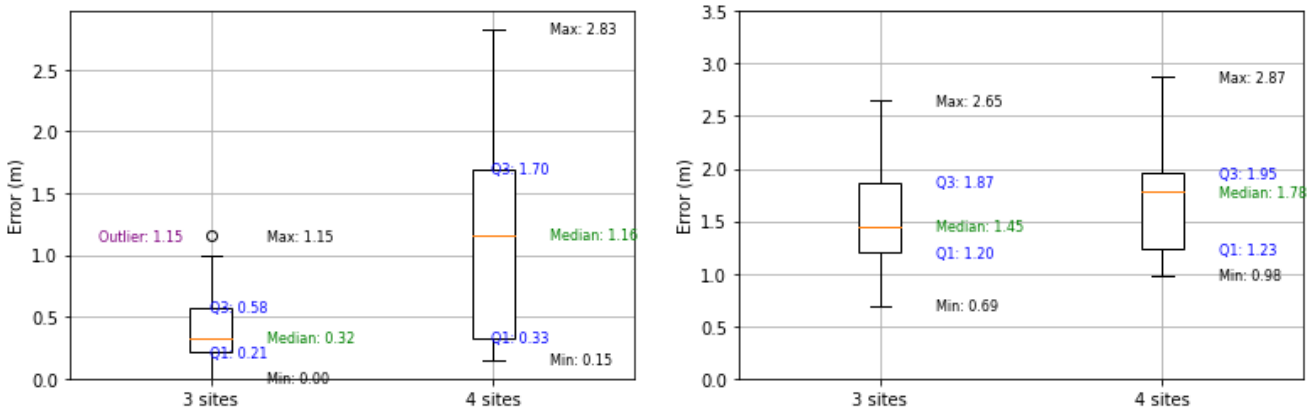

(a) (b)

FIGURE 21. Box-and-whisker plots for error distances in the conference room when using three and four reference RFID tag sites: (a) on-grid coordinates and (b) randomly chosen off-grid coordinates.

D. EVALUATING ACCURACY USING CLASSIFICATION ALGORITHMS

Classification algorithms based on label coordinates are also applicable in RFID-based localization systems. The label to be tested in this experiment is shown in Figs. 6 (b) and 7 (b).

There are two criteria for determining accuracy. Criteria 1: its success is measured by the ability to predict the position, including neighboring points. For example, in Fig. 18, Label 13 is considered successful if this point is predicted on labels included in the red rectangle. Criteria 2: accuracy is judged by whether the predicted label is on the ideal label or next to the nearest point.

From the evaluation results in Figs. 16 and 17, the decision tree algorithm produces the best accuracy.

The error map of the laboratory room off-grid using the decision tree algorithm is shown in Fig. 18. Based on the error map, the prediction of label F goes to label 11, meaning that label F is not included in the calculation of success rate in criteria 1 and 2.

E. PERFORMANCE COMPARISON OF TREE-BASED ALGORITHMS IN REGRESSION AND CLASSIFICATION

The tree-based algorithms (decision tree, random forest, and XGBoost) showed better performance than that of the CNN and linear regression. Although decision trees are typically applied to simple problems, the occurrence of overfitting may worsen performance of the decision tree algorithm [50]. Therefore, the decision tree algorithm showed the best performance in the classification and regression of the on-grid analysis in the conference room. However, for other regressions, decision tree algorithms showed worse performance. In contrast, the random forest and XGBoost, which employ ensemble averages of decision trees, showed better performance than did the decision tree because the ensemble average can eliminate overfitting problems. These studies concluded that evaluating tree-based algorithms, including decision trees, random forests, and XGBoost, is essential for effectively choosing the best algorithm for a target environment.

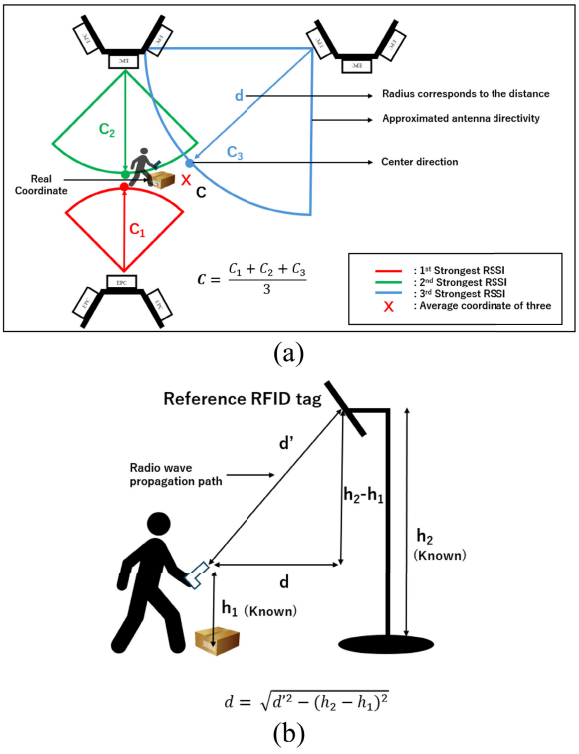

FIGURE 22. Location estimation based on distance decay. (a) Localization principle (b) Principle to obtain floor projected distance *d*.

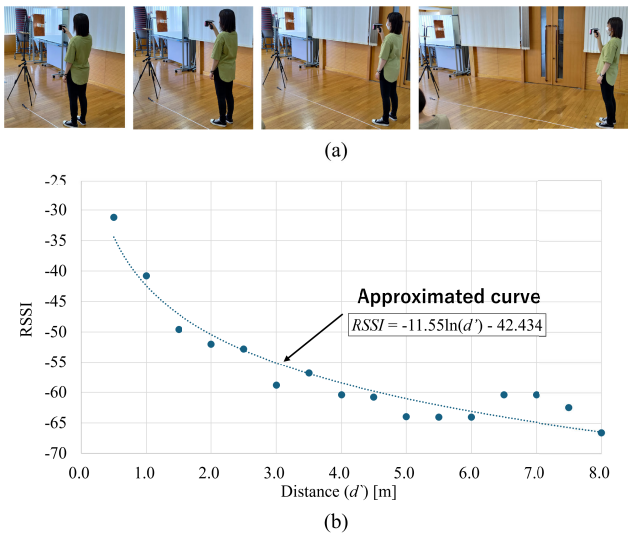

FIGURE 23. Relationship between the radio wave propagation distance and RSSI. (a) Experiment for calibration to determine the relationship between the RSSI and distance. (b) Approximated curve of the relationship.

F. EXPERIMENTAL RESULTS FOR FOUR REFERENCE RFID TAG SITES

Figure 19 shows the new experimental results obtained in the conference room after adding one more set of reference RFID tags (from #10 to #12). Figures 20 (a) and (b) show the error distance distribution maps for the on-grid and off-grid conditions, respectively, when regressions are applied using the random forest algorithm. Figures 21 (a) and (b) show box-and-whisker plots for the on-grid and off-grid conditions, respectively. Figures 21 (a) and (b) also compare the results for the cases using three (Figure 12 (a) and (b)) and four reference RFID tag sites. Min is the smallest observed value, Q1 is the first quartile, Median is the middle value, Q3 is the third quartile, and Max is the largest value. The outliers are significantly different from the other values in the dataset.

These comparative studies confirmed that increasing the number of reference RFID tag sites slightly decreases the localization accuracy because an increase in the number of sites increases the RSSI vector dimensions and complicates ML estimation problems. In addition, different arrangements of the reference RFID tag sites may lead to different performance. However, these results also verified that the proposed localization method worked well and provided acceptable results in a realistic indoor environment. This issue will be addressed in our future studies.

G. AREA ESTIMATION METHOD BASED ON THE DISTANCE DECAYS OF RSSIS

As a comparative study with the proposed ML-based localization method, this subsection evaluates the localization method on the basis of the distance decay of radio waves [27], [28]. The RSSIs of the reference RFID tags are measured by the handheld reader decay depending on the distances between them. This method provides approximated distances between the handheld reader and reference RFID tags, allowing localization in conjunction with the directivity of the reference RFID tags. This method considers the propagation channel to be a line-of-sight propagation path between the handheld RFID reader and reference RFID tags, ignoring the complex multipath propagation effects in indoor environments. This method may be a simple and effective area estimation method in non-multipath-rich environments such as conference rooms. In contrast, this method cannot provide reasonable area estimation performance in multipath-rich environments, such as the laboratory that was described in this paper. The advantage of this distance decay-based area estimation method is its simplicity of implementation because no fingerprint constructions are necessary in advance, as in the proposed ML-based method.

Figure 22 shows the area estimation method utilizing the distance decays of RSSIs instead of ML. Figure 22 (a) shows the area estimation principle of this method. The sectors represent the approximated antenna directivities of the reference RFID tags in the azimuth plane, and the radii correspond to the estimated distances. It should be noted that the goal of showing the sectors is to provide a comprehensive understanding for users, and the details of the sector shapes do not affect the area estimation accuracies. The colors indicate the magnitudes of the RSSIs. The antenna directivities of the reference RFID tags also provide representative directions as the centers of the antenna directivities. Distance decay-based distance estimation provides the distance d' between the reference RFID tag and the handheld RFID reader, as shown in Fig. 22 (b). The distance d in Fig. 22 (a) corresponds to

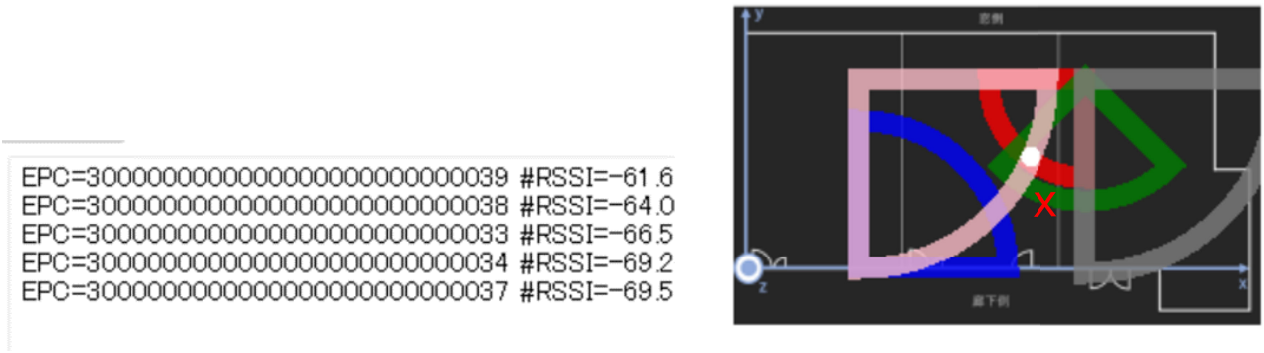

(a) (b)

FIGURE 24. Control software to determine the estimated location on the basis of distance decay in the conference room. (a) RSSI order (b) Sectors for three maximum RSSIs (red, green, blue), as explained in Fig. 22.

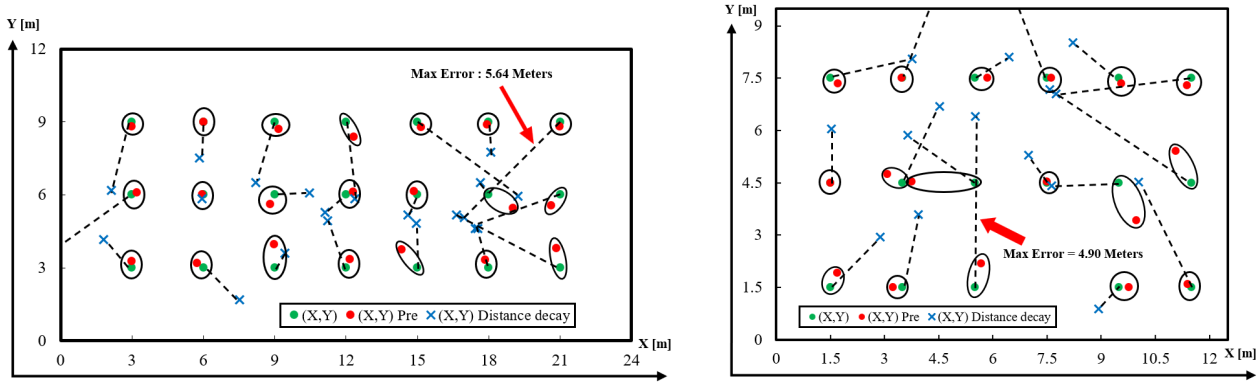

(a) (b)

FIGURE 25. Error distance maps of ML and distance decay in the (a) conference room and (b) laboratory.

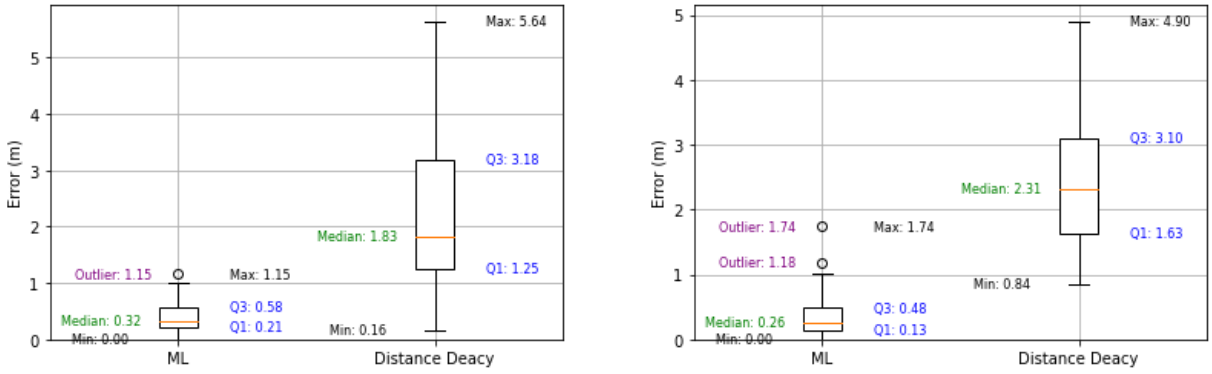

(a) (b)

FIGURE 26. Box-and-whisker plots for error distances between ML and distance decay in the (a) conference room and (b) laboratory.

the distance d in Fig. 22 (b) if a user directs the handheld RFID reader toward the reference RFID tag and assumes the known heights of the handheld RFID reader and reference RFID tag. The representative directions of the reference RFID tags antenna directivities and distances d point to the coordinates C_1, C_2 and C_3 in Fig. 22 (a), leading to an average coordinate C.

Figure 23 shows the experimentally obtained relationship between the RSSI and distance d', and the insets present the experimental environment. The dotted line provides the approximated curve of this relationship, and this approximated curve is given by

$$RSSI = -11.55 \ln d' - 42.434. \quad (1)$$

Transforming the above equation, we obtain the equation that is used to convert a measured RSSI value to a distance:

$$d' = e^{-\frac{RSSI+42.434}{11.55}}. \quad (2)$$

Figure 24 provides an example of the area estimation result based on the distance decay of the RSSI. Figure 24 (a) shows the EPC numbers of the reference RFID tags and their corresponding RSSI values in descending order. Figure 24 (b) provides an area estimation result computed by our developed software, corresponding to the illustrated area estimation principle shown in Fig. 22 (a). The distances derived from the three maximum RSSI values, the red, green, and blue sectors, and C_1, C_2 and C_3 lead to the average coordinate C represented by the red cross in Fig. 22 (b).

Figure 25 compares the distance errors of the distance decay-based method with those of the ML-based method. In this figure, the distance error of the distance decay-based method overlaps the previously shown figures: Fig. 12 (a) and 13 (a). Additional experiments in the conference room and laboratory were performed to produce error distance maps, as shown in Fig. 25 (a) and (b), respectively. Figure 26 shows box-and-whisker plots presenting comparative studies between the ML-based and distance decay-based methods. These additional experimental results confirmed that the error distances of the conference room are much shorter than those of the laboratory because the laboratory is a more highly multipath-rich environment compared with the conference room. However, the area estimation performance of the distance decay-based method is inferior to that of the ML-based method. These comparative studies revealed that the proposed ML-based method is necessary, especially in multipath-rich environments.

V. CONCLUSION

This paper introduces a simplified indoor localization system that uses a handheld RFID reader and the reference RFID tags with directional antenna radiation patterns using reflectors. These reference RFID tags provide RSSI and angle information, enabling localization in conference and laboratory rooms. A user with a handheld reader collects RSSI values by waving an arm and rotating the body to create a vector dataset. Known coordinates and on-grid RSSI datasets are utilized to train ML models. Both regression and classification algorithms were evaluated in this paper. Validation indicates that nine datasets are sufficient for the conference room, while 13 datasets are needed for the laboratory due to complex propagation and shadowing. Notably, in the conference room and laboratory room, the random forest regression algorithm was indicated to be the most effective for predicting coordinates, with maximum error distances of 1.15 m (on-grid) and 2.65 m (off-grid) in the conference room and 1.74 m (on-grid) and 2.53 m (off-grid) in the laboratory. The decision tree classification algorithm emerges as the most accurate for the conference and laboratory rooms.

ACKNOWLEDGMENT

The authors would like to thank Yangyu Park and Mayuri Horie for their contributions to this work.

REFERENCES

[1] E. Žunic, S. Delalic, K. Hodžic, A. Besirevic, and H. Hindija, "Smart warehouse management system concept with implementation," in *Proc. 14th Symp. Neural Netw. Appl. (NEUREL)*, Belgrade, Serbia, Nov. 2018, pp. 1–5, doi: 10.1109/NEUREL.2018.8587004.

[2] A. Polo, F. Viani, F. Robol, A. Massa, S. Marchesi, and L. Zappini, "Optimization strategies for fleet management based on wireless terminals localization in smart cities scenarios," in *Proc. IEEE Int. Smart Cities Conf.*, Sep. 2016, pp. 1–6, doi: 10.1109/ISC2.2016.7580851.

[3] J. Tang, Z. Gong, H. Wu, and B. Tao, "RFID-based pose estimation for moving objects using classification and phase-position transformation," *IEEE Sensors J.*, vol. 21, no. 18, pp. 20606–20615, Sep. 2021, doi: 10.1109/JSEN.2021.3098314.

[4] M. A. Fadzilla, A. Harun, and A. B. Shahriman, "Localization assessment for asset tracking deployment by comparing an indoor localization system with a possible outdoor localization system," in *Proc. Int. Conf. Comput. Approach Smart Syst. Design Appl. (ICASSDA)*, Kuching, Malaysia, Aug. 2018, pp. 1–6, doi: 10.1109/ICASSDA.2018.8477602.

[5] C. K. M. Lee, C. M. Ip, T. Park, and S. Y. Chung, "A Bluetooth location-based indoor positioning system for asset tracking in warehouse," in *Proc. IEEE Int. Conf. Ind. Eng. Eng. Manage. (IEEM)*, Macao, China, Dec. 2019, pp. 1408–1412, doi: 10.1109/IEEM44572.2019.8978639.

[6] S. Lopez-Soriano and J. Parrón, "Performance assessment of a novel miniaturized RFID tag for inventorying and tracking metallic tools," *IEEE J. Radio Freq. Identificat.*, vol. 2, no. 3, pp. 127–133, Sep. 2018, doi: 10.1109/JRFID.2018.2868780.

[7] L. Chen, S. Thombre, K. Järvinen, E. S. Lohan, A. Alén-Savikko, H. Leppäkoski, M. Z. H. Bhuiyan, S. Bu-Pasha, G. N. Ferrara, S. Honkala, J. Lindqvist, L. Ruotsalainen, P. Korpisaari, and H. Kuusniemi, "Robustness, security and privacy in location-based services for future IoT: A survey," *IEEE Access*, vol. 5, pp. 8956–8977, 2017, doi: 10.1109/ACCESS.2017.2695525.

[8] T. T. Dinh, N.-S. Duong, and K. Sandrasegaran, "Smartphone-based indoor positioning using BLE iBeacon and reliable lightweight fingerprint map," *IEEE Sensors J.*, vol. 20, no. 17, pp. 10283–10294, Sep. 2020, doi: 10.1109/JSEN.2020.2989411.

[9] Z. Zhang, G. Xu, and E. C. Kan, "Outlooks for UHF RFID-based autonomous retails and factories," *IEEE J. Radio Freq. Identificat.*, vol. 7, no. 2, pp. 12–19, Apr. 2023, doi: 10.1109/JRFID.2022.3211474.

[10] R. Huo, S. Zeng, Z. Wang, J. Shang, W. Chen, T. Huang, S. Wang, F. R. Yu, and Y. Liu, "A comprehensive survey on blockchain in industrial Internet of Things: Motivations, research progresses, and future challenges," *IEEE Commun. Surveys Tuts.*, vol. 24, no. 1, pp. 88–122, 1st Quart., 2022, doi: 10.1109/COMST.2022.3141490.

[11] J. A. Rodger, "Forecasting of radio frequency identification entropy viscosity parking and forwarding algorithm flow risks and costs: Integrated supply chain health manufacturing system (ISCHMS) approach," *IEEE J. Radio Freq. Identificat.*, vol. 1, no. 4, pp. 267–278, Dec. 2017, doi: 10.1109/JRFID.2018.2795801.

[12] A. Abdelnour, F. Buchin, D. Kaddour, and S. Tedjini, "Improved traceability solution based on UHF RFID for cheese production sector," *IEEE J. Radio Freq. Identificat.*, vol. 2, no. 2, pp. 68–72, Jun. 2018, doi: 10.1109/JRFID.2018.2847241.

[13] Y. Zhang, Z. Guo, J. Lv, and Y. Liu, "A framework for smart production-logistics systems based on CPS and industrial IoT," *IEEE Trans. Ind. Informat.*, vol. 14, no. 9, pp. 4019–4032, Sep. 2018, doi: 10.1109/TII.2018.2845683.

[14] Z. Shen, X. Dong, Q. Fang, G. Xiong, C.-C. Ge, and F.-Y. Wang, "Parallel additive manufacturing systems," *IEEE J. Radio Freq. Identificat.*, vol. 6, no. 2, pp. 758–763, Apr. 2022, doi: 10.1109/JRFID.2022.3215600.

[15] D. K. Hadi, P. B. Santoso, and Sucipto, "Traceability implementation based on RFID at agro-industry: A review," *IOP Conf. Ser. Earth Environ. Sci.*, vol. 230, no. 1, Feb. 2019, Art. no. 012070.

[16] M. Kokkonen, S. Myllymäki, J. Putaala, and H. Jantunen, "A resonator enhanced UHF RFID antenna cable for inventory and warehouse applications," *IEEE J. Radio Freq. Identificat.*, vol. 6, no. 2, pp. 128–133, Apr. 2022, doi: 10.1109/JRFID.2021.3135047.

[17] K. Mannar, D. Ceglarek, F. Niu, and B. Abifaraj, "Fault region localization: Product and process improvement based on field performance and manufacturing measurements," *IEEE Trans. Autom. Sci. Eng.*, vol. 3, no. 4, pp. 423–439, Oct. 2006, doi: 10.1109/TASE.2006.880526.

[18] P. Wen and W. Cao, "Real-time job-shop scheduling model based on RFID," in *Proc. 2nd IEEE Int. Conf. Comput. Intell. Appl. (ICCIA)*, Sep. 2017, pp. 204–208, doi: 10.1109/CIAPP.2017.8167208.

[19] S. D'Avella, M. Unetti, and P. Tripicchio, "RFID gazebo-based simulator with RSSI and phase signals for UHF tags localization and tracking," *IEEE Access*, vol. 10, pp. 22150–22160, 2022, doi: 10.1109/ACCESS.2022.3152199.

[20] J.-M. Choi, K. Kim, and S.-C. Kim, "Outdoor localization based on RSS ranging aided by pedestrian dead reckoning in GPS restricted scenario," in *Proc. IEEE VTS Asia Pacific Wireless Commun. Symp. (APWCS)*, May 2022, pp. 186–190, doi: 10.1109/APWCS55727.2022.9906494.

[21] U. Ketprom, C. Mitrpant, P. Makhapun, S. Makwimanloy, and S. Laokok, "RFID for cattle traceability system at animal checkpoint," in *Proc. Annu. SRII Global Conf.*, Mar. 2011, pp. 517–521, doi: 10.1109/SRII.2011.107.

[22] C.-Y. Wan, C. Tanriover, and R. C. Shah, "Utilizing RFID tag motion detection in high tag density environments for customer browsing insights," *IEEE J. Radio Freq. Identificat.*, vol. 5, no. 4, pp. 345–356, Dec. 2021.

[23] Z. Liu, Z. Fu, T. Li, I. H. White, R. V. Penty, X. Yang, R. Du, and M. Crisp, "A phase and RSSI-based method for indoor localization using passive RFID system with mobile platform," *IEEE J. Radio Freq. Identificat.*, vol. 6, no. 2, pp. 544–551, Apr. 2022, doi: 10.1109/JRFID.2022.3179620.

[24] W. Shi, Y. Guo, S. Yan, Y. Yu, P. Luo, and J. Li, "Optimizing directional reader antennas deployment in UHF RFID localization system by using a MPCSO algorithm," *IEEE Sensors J.*, vol. 18, no. 12, pp. 5035–5048, Jun. 2018, doi: 10.1109/JSEN.2018.2832216.

[25] A. G. Dimitriou, "Design, analysis, and performance evaluation of a UHF RFID forward-link repeater," *IEEE J. Radio Freq. Identificat.*, vol. 4, no. 2, pp. 73–82, Jun. 2020, doi: 10.1109/JRFID.2019.2953785.

[26] M. Lalkota, G. Gupta, V. K. Pandit, and A. R. Harish, "UHF reader antenna system for near and far-field RFID operation," *IEEE J. Radio Freq. Identificat.*, vol. 3, no. 1, pp. 14–24, Mar. 2019, doi: 10.1109/JRFID.2018.2884935.

[27] J. Xu, Z. Li, K. Zhang, J. Yang, N. Gao, Z. Zhang, and Z. Meng, "The principle, methods and recent progress in RFID positioning techniques: A review," *IEEE J. Radio Freq. Identificat.*, vol. 7, no. 2, pp. 50–63, Apr. 2023, doi: 10.1109/JRFID.2022.3233855.

[28] C. Li, L. Mo, and D. Zhang, "Review on UHF RFID localization methods," in *IEEE J. Radio Freq. Identificat.*, vol. 3, no. 4, pp. 205–215, Dec. 2019, doi: 10.1109/JRFID.2019.2924346.

[29] Y. M. Madany, D. A. E. Mohamed, W. A. E. Ali, and R. F. Emara, "Modelling and simulation of indoor reverse RFID tag localization method based on mobile antenna reader position," in *Proc. UKSim-AMSS 19th Int. Conf. Comput. Model. Simul. (UKSim)*, Apr. 2017, pp. 235–239.

[30] H. Zhang and C. Ye, "An indoor wayfinding system based on geometric features aided graph SLAM for the visually impaired," *IEEE Trans. Neural Syst. Rehabil. Eng.*, vol. 25, no. 9, pp. 1592–1604, Sep. 2017, doi: 10.1109/TNSRE.2017.2682265.

[31] L. Cocco, K. Mannaro, R. Tonelli, L. Mariani, M. B. Lodi, A. Melis, M. Simone, and A. Fanti, "A blockchain-based traceability system in agri-food SME: Case study of a traditional bakery," *IEEE Access*, vol. 9, pp. 62899–62915, 2021, doi: 10.1109/ACCESS.2021.3074874.

[32] S. Subedi, E. Pauls, and Y. D. Zhang, "Accurate localization and tracking of a passive RFID reader based on RSSI measurements," *IEEE J. Radio Freq. Identificat.*, vol. 1, no. 2, pp. 144–154, Jun. 2017, doi: 10.1109/JRFID.2017.2765618.

[33] B. D. B. Chowdhury, S. Masoud, Y.-J. Son, C. Kubota, and R. Tronstad, "A dynamic HMM-based real-time location tracking system utilizing UHF passive RFID," *IEEE J. Radio Freq. Identificat.*, vol. 6, no. 2, pp. 41–53, Apr. 2022, doi: 10.1109/JRFID.2021.3102507.

[34] A. Mostaccio, G. M. Bianco, G. Marrocco, and C. Occhiuzzi, "RFID technology for food industry 4.0: A review of solutions and applications," *IEEE J. Radio Freq. Identificat.*, vol. 7, no. 2, pp. 145–157, Apr. 2023, doi: 10.1109/JRFID.2023.3278722.

[35] E.-T. Bouali, M. R. Abid, E.-M. Boufounas, T. A. Hamed, and D. Benhaddou, "Renewable energy integration into cloud & IoT-based smart agriculture," *IEEE Access*, vol. 10, pp. 1175–1191, 2022, doi: 10.1109/ACCESS.2021.3138160.

[36] G. Xu, P. Sharma, D. L. Hysell, and E. C. Kan, "Indoor object sensing using radio-frequency identification with inverse methods," *IEEE Sensors J.*, vol. 22, no. 12, pp. 11336–11344, Jun. 2022, doi: 10.1109/JSEN.2021.3086700.

[37] Y. Ma, Y. Zhang, B. Wang, and W. Ning, "SCLA-RTI: A novel device-free multi-target localization method based on link analysis in passive UHF RFID environment," *IEEE Sensors J.*, vol. 21, no. 3, pp. 3879–3887, Feb. 2021, doi: 10.1109/JSEN.2020.3023096.

[38] L. Talbi and G. Y. Delisle, "Using directive antennas to reduce multipath fading in indoor PCN systems," in *IEEE Antennas Propag. Soc. Int. Symposium. Dig.*, vol. 4, May 1999, pp. 2448–2451, doi: 10.1109/APS.1999.789305.

[39] A. Motroni, F. Bernardini, A. Buffi, P. Nepa, and B. Tellini, "A UHF-RFID multi-antenna sensor fusion enables item and robot localization," *IEEE J. Radio Freq. Identificat.*, vol. 6, pp. 456–466, Apr. 2022, doi: 10.1109/JRFID.2022.3166354.

[40] A. Tzitzis, A. Filotheou, A. R. Chatzistefanou, T. Yioultsis, and A. G. Dimitriou, "Real-time global localization of a mobile robot by exploiting RFID technology," *IEEE J. Radio Freq. Identificat.*, vol. 7, no. 1, pp. 486–506, Apr. 2023, doi: 10.1109/JRFID.2023.3288982.

[41] Z. Liu, Z. Fu, T. Li, I. H. White, R. V. Penty, and M. Crisp, "An ISAR-SAR based method for indoor localization using passive UHF RFID system with mobile robotic platform," *IEEE J. Radio Freq. Identificat.*, vol. 5, no. 4, pp. 407–416, Dec. 2021, doi: 10.1109/JRFID.2021.3097803.

[42] A. R. Chatzistefanou, G. Sergiadis, and A. G. Dimitriou, "Tag localization by handheld UHF RFID reader with optical and RFID landmarks," *IEEE J. Radio Freq. Identificat.*, vol. 7, no. 2, pp. 330–340, Apr. 2023, doi: 10.1109/JRFID.2023.3238822.

[43] J. D. Kraus and R. J. Marhefka, *Antennas*. New York, NY, USA: McGraw-Hill, 2003, ch. 1, pp. 347–350.

[44] J. Bi, J. Wang, H. Cao, G. Yao, Y. Wang, Z. Li, M. Sun, H. Yang, J. Zhen, and G. Zheng, "Inverse distance weight-assisted particle swarm optimized indoor localization," *Appl. Soft Comput.*, vol. 164, Oct. 2024, Art. no. 112032.

[45] Y. Yang, L. Zhang, J. Xu, D. Li, J. Bao, and J. Tan, "Cooperative indoor localization system based UWB and random forest algorithm in complicated underground NLOS scenario," in *Proc. 9th International Conference on Digital Home (ICDH)*, 2022, pp. 271–276, doi: 10.1109/ICDH57206.2022.00049.

[46] B. Yang, Y. He, H. Liu, Y. Chen, and Z. Jin, "A lightweight fault localization approach based on XGBoost," in *Proc. IEEE 20th Int. Conf. Softw. Qual., Rel. Secur. (QRS)*, Dec. 2020, pp. 168–179, doi: 10.1109/QRS51102.2020.00033.

[47] N. Bouchiba and A. Kaddouri, "Fault detection and localization based on decision tree and support vector machine algorithms in electrical power transmission network," in *Proc. 2nd Int. Conf. Adv. Electr. Eng. (ICAEE)*, Constantine, Algeria, Oct. 2022, pp. 1–6, doi: 10.1109/ICAEE53772.2022.9961970.

[48] A. A. Pimentel and R. G. Baldovino, "IoT indoor localization using design of experiment analysis and multi-output regression models," in *Proc. IEEE Int. Power Renew. Energy Conf.*, Dec. 2022, pp. 1–5, doi: 10.1109/IPRECON55716.2022.10059563.

[49] H. Chen, Y. Zhang, W. Li, X. Tao, and P. Zhang, "ConFi: Convolutional neural networks based indoor Wi-Fi localization using channel state information," *IEEE Access*, vol. 5, pp. 18066–18074, 2017, doi: 10.1109/ACCESS.2017.2749516.

[50] P. Mahalingam, D. Kalpana, and T. Thyagarajan, "Overfit analysis on decision tree classifier for fault classification in DAMADICS," in *Proc. IEEE Madras Sect. Conf. (MASCON)*, Aug. 2021, pp. 1–4, doi: 10.1109/MASCON51689.2021.9563557.

DANANG KUMARA HADI received the M.T. degree in agroindustrial technology from Universitas Brawijaya, Malang, Indonesia, in 2019, and the Ph.D. degree in society's infrastructure system science from Ibaraki University, Japan, in 2023. He is currently a Lecturer with the Agroindustrial Technology Department, Faculty of Agriculture, Universitas Muhammadiyah Jember, Indonesia. His research interests include agroindustrial systems based on RFID sensors and technology of food traceability systems.

ZEQUN SONG received the M.E. degree in science and engineering from Ibaraki University, Japan, in 2022, where he is currently pursuing the Ph.D. degree with the Graduate School of Science and Engineering. He was awarded the Highly Commended Paper Award from the International Telecommunication Networks and Application Conference (ITNAC) 2021.

BUDI RAHMADYA (Member, IEEE) received the M.E. degree in computer science from the Nara Institute of Science and Technology (NAIST), Ikoma, Japan, in 2013, and the Ph.D. degree in computer and information science from Ibaraki University, Japan, in 2021. He is currently a Lecturer with the Computer System Department, Faculty of Information and Technology, Andalas University, Padang, Indonesia. His research interests include wireless communications, low power wide area networks (LPWAN), sensor networks, and networking.

SHOGO KOZUME received the B.E. degree in engineering from Ibaraki University, Japan, in 2023, where he is currently pursuing the M.E. degree with the Graduate School of Science and Engineering.

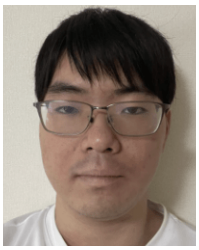

TOMONORI SUMIYA received the B.E. degree in engineering from Ibaraki University, Japan, in 2024, where he is currently pursuing the M.E. degree with the Graduate School of Science and Engineering.

RAN SUN (Member, IEEE) received the B.E., M.E., and Ph.D. degrees in computer and information science from Ibaraki University, Japan, in 2016, 2017, and 2020, respectively. Since 2020, he has been an Assistant Professor with Ibaraki University. His research interests include optical wireless communication, error-correcting codes, the Internet of Things platform, and vehicle-borne radar. He is a member of the Institute of Electronics, Information and Communication Engineers (IEICE).

SHIGEKI TAKEDA (Member, IEEE) received the B.E., M.E., and Ph.D. degrees in electrical and electronic engineering from Tottori University, Tottori, Japan, in 1996, 1998, and 2000, respectively. Since 2000, he has been with the Department of Media and Telecommunications Engineering, College of Engineering, Ibaraki University, Japan, where he is currently a Professor. His research interests include radio-frequency identification (RFID) tags and antenna systems.

XIAOYAN WANG (Senior Member, IEEE) received the B.E. degree from Beihang University, China, and the M.E. and Ph.D. degrees from the University of Tsukuba, Japan. From 2013 to 2016, he was an Assistant Professor (by special appointment) with the National Institute of Informatics, Japan. He is currently an Associate Professor with the Graduate School of Science and Engineering, Ibaraki University, Japan. His research interests include intelligent networking, wireless communications, cloud computing, and big data systems.